4α-Phorbol negates the inhibitory effects of phorbol-12-myristate-13-acetate on human cilia and alters the phosphorylation of PKC

Xowi K.M.S. Mwimbi, Richmond Muimo, Kate J. Treharne, Gibson Sijumbila, Michael Green, Anil Mehta*

Tayside Institute of Child Health, Ninewells Hospital and Medical School, University of Dundee, Dundee DD1 9SY, UK

Received 18 June 2002; revised 27 August 2002; accepted 28 August 2002

First published online 11 September 2002

Edited by Veli-Pekka Lehto

Abstract In medium 199, ciliary beat frequency (CBF) in human nasal epithelium declines to 60% of baseline by 2 h and 1 nM phorbol-12-myristate-13-acetate (PMA) doubles the rate of decline by activating protein kinase C (PKC). We find that a reported negative control for PMA, 4α-phorbol (1 pM–1 nM) ± 1 nM PMA, not only maintains CBF at baseline, but arrests a pre-existing PMA-induced decline in CBF and alters the profile of multiple phosphorylated PKC species. Thus, 4α-phorbol not only potently prevents PMA from inhibiting CBF but also has potent effects on the phosphorylation of PKC.

Key words: Lung; Phorbol ester; Ciliary beat frequency

1. Introduction

Protein kinase C (PKC) regulates signal transduction across cell membranes. The study of this enzyme is facilitated by use of phorbol esters, plant-derived, potent activators of the C1 domains within some PKC species [1–7]. In the concluding sentence of their recent review on PKC regulation, Kazanietz et al. [8] state that ''our challenge is to decipher the molecular mechanisms responsible for such a complex regulation''. In this study, we challenge a commonly held axiom in phorbol ester cell biology concerning the assumed inactivity of one class of phorbol controls and provide further insight into the complexity of PKC regulation in human airway epithelium.

In lung, PKC regulates mucociliary clearance, that process by which airway mucus is removed by the beating action of cilia [9–10]. The in vitro study of cilia provides a quasi-real time bioassay of PKC function because phorbol esters reduce airway ciliary beat frequency (CBF) across species (for example, rabbit [11]; sheep [12]; dog [13]; human, this study and [14]). When phorbol esters such as 4β,9α,12β,13α,20-pentahydroxytiglia-1,6-dien-3-one 12β-myristate-13-acetate (phorbol-12-myristate-13-acetate; PMA) and 12-*O*-tetradecanoylphorbol-13-acetate (TPA) are used as PKC activators [15–17], it is an accepted practice to apply the stereo-isomer 4α,9α,12β,13α,20-pentahydrotiglia-1,6-dien-3-one (4α-PHR; isophorbol) as a negative control because it is considered not to activate PKC in vitro [18,19]. Here, we show that 4α-PHR has a potent inhibitory activity on a PMA-induced decline in CBF in whole cells. We provide evidence that the profile of phosphorylated PKC species is differentially modulated by 4α-PHR suggesting that this compound can affect PKC activity in intact cells.

2. Materials and methods

2.1. Materials

All reagents used were of analytical grade and included PMA, 4α-PMA (inactive PMA control), and dimethyl sulfoxide (DMSO), which were obtained from Sigma (Poole, UK), 4α-PHR (isophorbol), the cell-permeable, myristoylated, selective PKC inhibitor EGF-R Fragment 651-658 (MyrPKCI) [5,20–23], and bisindolylmaleimide I (BIMI), from Calbiochem-Novabiochem (Nottingham, UK), and medium 199 (M199), from ICN Biochemicals (Oxfordshire, UK). The phorbol esters (4α-PHR, 4α-PMA and PMA) were dissolved in DMSO first before being diluted to the desired concentrations in M199. Isoform specific phospho-PKC antibodies were purchased from NEB (Hitchin, UK).

2.2. Subject selection

Human nasal epithelial cells (HNE) were obtained from normal volunteers or immediately after the induction of general anaesthesia from non-asthmatic, non-atopic patients undergoing routine operations unrelated to nasal disease (age range, 10–45 years). These patients had had no respiratory infections for at least a month prior to the date of operation. Approval for the study was given by the Tayside Committee on Medical Research Ethics and informed written consent was obtained from the volunteers, patients and parents of minors in all cases.

2.3. Sample collection

This has been described in detail elsewhere [24,25]. Briefly, strips of ciliated HNE were obtained with a cytology brush from the inferior turbinate, placed in culture medium (M199) and loaded into a perfusion chamber.

2.4. Measurement of CBF

This has been described in detail elsewhere [14,26–29]. Briefly, CBF was measured at the normal physiological nasal temperature (32 ± 0.5°C) using our well-characterised video-based, Hoffman contrast technique (Brian Reece Scientific, Newbury Berks). An aliquot of cells was transferred in M199 to a glass-walled modified Rose chamber with an internal volume of 0.5 ml. The chamber was then connected to a syringe-operating non-peristaltic infusion pump (Medfusion Model 2010, Medex Medical Inc., Lancashire, UK) which

*Corresponding author. Fax: (44)-1382-632597.
E-mail address: a.mehta@dundee.ac.uk (A. Mehta).

Abbreviations: M199, medium 199; PKC, protein kinase C; CBF, ciliary beat frequency; PMA, phorbol-12-myristate-13-acetate; 4α-PHR, 4α,9α,12β,13α,20-pentahydrotiglia-1,6-dien-3-one; 4α-PMA, inactive PMA control; BIMI, bisindolylmaleimide I; MyrPKCI, myristoylated peptide inhibitor of PKC; HNE, human nasal epithelial cells

0014-5793/02/$22.00
PII: S0014-5793(02)03358-6

delivered 2.5 ml of the relevant test solution at a rate of 0.125 ml min^{-1}. This rate of infusion eliminated changes in CBF which would have been induced by higher perfusion rates as found in previous studies [14,25,30]. All readings were taken in the absence of flow. The first post-perfusion CBF measurements were taken within 30 s of the termination of the flow of fluid. The pH of all solutions used was between 7.2 and 7.4, a range known not to adversely affect ciliary activity [31]. The protocol involved incubation of HNE in the relevant solution during which HNE were selected at random and CBF recorded from the same point on the ciliated cell border. The baseline CBF was established by taking readings every 5 min for 30 min, before the chamber was perfused using the infusion pump, and CBF readings continued (after the end of the perfusion) until the 120th min.

2.5. Experimental CBF protocols with test solutions

HNE were maintained at 32°C and CBF profiles were established to test the effects of PKC activation or PKC inhibition (Fig. 1), or with different combinations of inhibitors (Fig. 2). In separate experiments (Fig. 3), reagents were changed after baseline and PKC-manipulated CBF profiles had been taken over the first 30 min, to determine whether the effects on CBF were reversible.

In Fig. 1, CBF was recorded under zero flow conditions in M199 (closed circles, $n=32$), 1 nM 4α-PHR (phorbol control, open squares, $n=33$) or 1 nM PMA (open, upward-pointing triangles, $n=49$). Fig. 2 shows the effects of 10 μM MyrPKCI alone (specific PKC blocker, open downward-pointing triangles, $n=24$), a mixture of 10 μM MyrPKCI+1 nM PMA (to test the ability of this peptide to suppress the inhibitory effect of PMA on CBF, open diamonds, $n=22$), 1 nM 4α-PMA (a myristoylated, phorbol control for PMA, open hexagons, $n=13$), or 100 nM BIMI (a selective classical, and partial novel PKC isoform blocker [32–35], closed, downward-pointing triangles, $n=21$).

In further perfusion experiments (Fig. 3), baseline CBF was recorded in 1 nM PMA for 30 min, before perfusing the cells with fresh 1 nM PMA at a rate of 0.125 ml min^{-1} over 20 min (open triangles, $n=12$). CBF readings were taken after the cessation of flow, up to the 120th min. Separately, HNE were observed in 1 nM PMA for 30 min, before perfusing a mixture of 1 nM PMA and 1 nM 4α-PHR at the same rate (closed diamonds, $n=12$). CBF profiles were also determined for cells exposed to 1 nM 4α-PHR before being perfused with the PMA+4α-PHR mixture for 20 min as for the other series (open squares, $n=12$). Finally, HNE were observed in 1 nM PMA for 30 min, before the mixture of 1 nM PMA+10 μM MyrPKCI was perfused at the same rate as the other series (open diamonds, $n=25$).

Dose–response studies were carried out under zero flow conditions using increasing concentrations of 4α-PHR in mixture with 1 nM PMA, whose results are summarised in Fig. 4, for 1 fM ($n=16$ cell borders), 10 fM ($n=15$), 100 fM ($n=16$), 1 pM ($n=16$), 10 pM ($n=12$) and 100 pM ($n=6$) of 4α-PHR.

2.6. Data analysis

Initial CBF readings varied widely within and between patients (4.7–16.1 Hz). As previously described [14], CBF was therefore expressed as a percentage of the first (i.e. time 0), baseline reading, for all experiments. Significance of difference between reagent series was accepted at $P<0.05$, using regression analysis.

2.7. Western blots

To determine whether 4α-PHR regulated the phosphorylation of PKC, HNE collected as described above were incubated at 32°C for 30 min in M199 ± PMA (1 nM), 4α-PHR (1 nM) or PMA+4α-PHR (1 nM each). The 30 min time point was used because it represented the earliest time point showing a significant difference in CBF between 4α-PHR and the other reagents. The cells were then washed twice in 1×PBS containing the above reagents to remove M199 prior to storage in liquid N_2. HNE were then sonicated in HEPES buffer, pH 7.5, containing 1% *N*-octyl-β-D-glucopyranoside, sodium fluoride (50 mM), sodium pyrophosphate (5 mM), EDTA (1 mM), dithiothreitol (1 mM), protease inhibitors (1 tablet/50 ml pefabloc, Boehringer Mannheim), okadaic acid (1 μM), microcystin LR (10 μM) and benzamidine (1 mM). Proteins separated by SDS–PAGE (50 μg per lane) were transferred to PVDF membrane (Millipore) by semi-dry electrophoretic transfer (Pharmacia) using 0.8 mA/cm^2 for 1 h with 20% methanol added to standard SDS–PAGE running buffer. Pre-stained markers were used to confirm transfer. The blots were probed with phospho-PKC primary antibodies (1:1000), non-phospho isoform specific antibodies and horseradish peroxidase-conjugated anti-rabbit secondary antibody (1:2000) followed by supersignal chemiluminescence detection (Pierce).

3. Results

3.1. Manipulation of PKC generates a complex CBF response

Cilia observed without fluid-flow in M199 (Fig. 1) showed a steady decline in CBF from 10.1 ± 0.4 Hz (mean ± S.E.M., $n=32$; range 5.8–12.9 Hz), to 60 ± 7% of the baseline, by 2 h. In contrast, CBF fell significantly faster in the presence of 1 nM PMA (Figs. 1 and 2, open upward-pointing triangles) from baselines of 9.9 ± 0.4 Hz (Fig. 1, $n=49$; range 6.5–14.1 Hz) and 12.0 ± 0.5 Hz (Fig. 2, $n=11$; range 7.6–13.7 Hz) to 29 ± 5% and 25 ± 5% of baseline, respectively, by 2 h. The difference between the rates of CBF decline in M199 alone versus 1 nM PMA was highly significant ($P<0.001$). Additionally, the pattern of CBF decline with PMA was noticeably biphasic, the CBF falling very rapidly initially, followed by a slower rate of decline after a point of inflexion around the end of the first hour. In contrast, CBF remained at baseline levels, albeit with oscillations throughout the experiment, both when MyrPKCI was applied alone (Fig. 2, $n=24$; open downward-pointing triangles, 7.6 ± 0.3 Hz, range 4.1–10.3 Hz), and when combined with 1 nM PMA (Fig. 2, $n=22$; open diamonds, 13.5 ± 0.3 Hz, range 10.5–15.5 Hz). The latter finding confirmed that MyrPKCI was dominant over PMA. Unexpectedly, attempts to reproduce this stability of baseline CBF by partial blockade of PKC with 100 nM BIMI were unsuccessful, and CBF declined in a steady manner (without a point of inflexion seen with PMA) from a baseline of 11.8 ± 0.4 Hz (Fig. 2, $n=21$; closed downward-pointing triangles, range 6.5–14.8 Hz) to end at 26 ± 5% of baseline by 2 h. The main difference between the pattern of decline with BIMI and PMA lay in the initial rate of decline, which was faster in PMA. This significant difference in pattern between BIMI and PMA profiles is best observed by comparing the CBF between the 40th and 85th min ($P<0.001$). However, over the whole 2 h, BIMI gave a similar percentage decline to PMA ($P>0.1$, by regression analysis). Thus we observe the paradox that a PKC

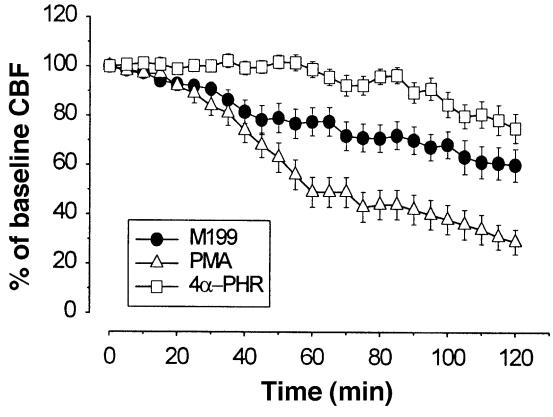

Fig. 1. Differential effects of 4α-PHR and PMA on CBF at 32°C. The CBF response in M199 alone ($n=32$) was compared to that in 1 nM PMA ($n=49$), and the 'inactive' control phorbol 1 nM 4α-PHR ($n=33$). The CBF profiles were significantly different from each other ($P<0.001$, by regression analysis). The stabilising effect of the 'inactive' phorbol above medium control was unexpected.

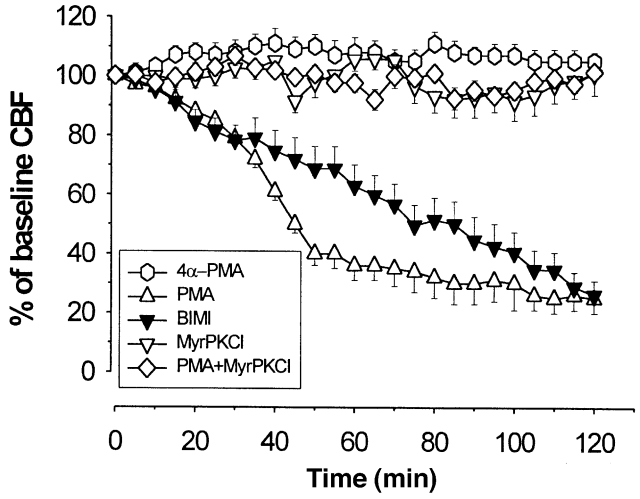

Fig. 2. Further manipulation of PKC activity and the CBF response. Time courses are shown in 10 μM MyrPKCI ($n=24$), 1 nM PMA ($n=11$), 1 nM 4α-PMA ($n=13$), 100 nM BIMI ($n=21$), and a 10 μM MyrPKCI and 1 nM PMA mixture ($n=22$). The CBF remained around baseline levels in 4α-PMA, MyrPKCI, and PMA+MyrPKCI ($P>0.1$). CBF declined significantly in BIMI, while PMA induced the expected rapid decline in CBF within the first hour ($P<0.001$, by regression analysis compared to MyrPKCI ± PMA or 4α-PMA).

activator (PMA) and a selective PKC inhibitor (BIMI) both decrease CBF, albeit with different profiles, whereas a PMA-dominant inhibitor of PKC, MyrPKCI, has the reverse effect ± PMA. These anomalous results were accompanied by a further puzzle because the 'control' phorbol compound 1 nM 4α-PHR also stabilised CBF at baseline levels (9.0 ± 0.4 Hz; range 6.0–11.5 Hz) for up to 90 min, but thereafter, CBF only declined to 75 ± 6%, by 2 h (Fig. 1, open squares, $n=33$). This relatively stable 4α-PHR-dependent profile remained significantly above M199 ± PMA throughout ($P<0.001$). This stabilising effect on CBF was also observed with the apparently 'inactive' 4α-PMA (Fig. 2, 10.9+0.3 Hz; range 8.8–14.5 Hz, open hexagons, $n=13$) that also contains the myristoylated tail present in PMA, suggesting that the structure at the fourth carbon was the critical factor governing the differential response between 4α-PHR and PMA. We tested the simplest interpretation of these anomalous results, that the supposedly inactive compound, 4α-PHR, blocked PMA-mediated inhibition of CBF, by using serial perfusions of 4α-PHR, MyrPKCI and PMA (Fig. 3).

3.2. Serial reagent perfusions

When cilia were pre-incubated for 30 min in 1 nM PMA (baseline CBF 11.7 ± 0.6 Hz; range 8.7–14.9 Hz), before perfusing an equimolar solution of 1 nM 4α-PHR+PMA, the CBF fell rapidly only up to the point when the 4α-PHR+PMA mixture was added (Fig. 3, closed diamonds, $n=12$). This showed that 4α-PHR was dominant over PMA. The arrest in decline of CBF (at 53 ± 3% of the baseline) remained until the end of the experiment. In the reverse experimental protocol, cilia were pre-incubated in 4α-PHR (Fig. 3, open squares, $n=12$; baseline CBF 11.3 ± 0.7 Hz; range 6.1–14.7 Hz) prior to the addition of the equimolar (1 nM) mixture of 4α-PHR+PMA. This time, the CBF did not decline significantly from baseline for the duration of the study (96 ± 6% of the baseline by 2 h), confirming that the 4α-PHR was dominant over the PMA-induced decline in CBF. This was not an artefact because in control experiments where cilia were pre-incubated in PMA (Fig. 3, open upward-pointing triangles, $n=12$; baseline CBF 12.4 ± 0.6 Hz; range 9.8–16.1 Hz), before perfusing fresh PMA, the CBF continued its original path of descent reaching 20 ± 4% of the baseline by

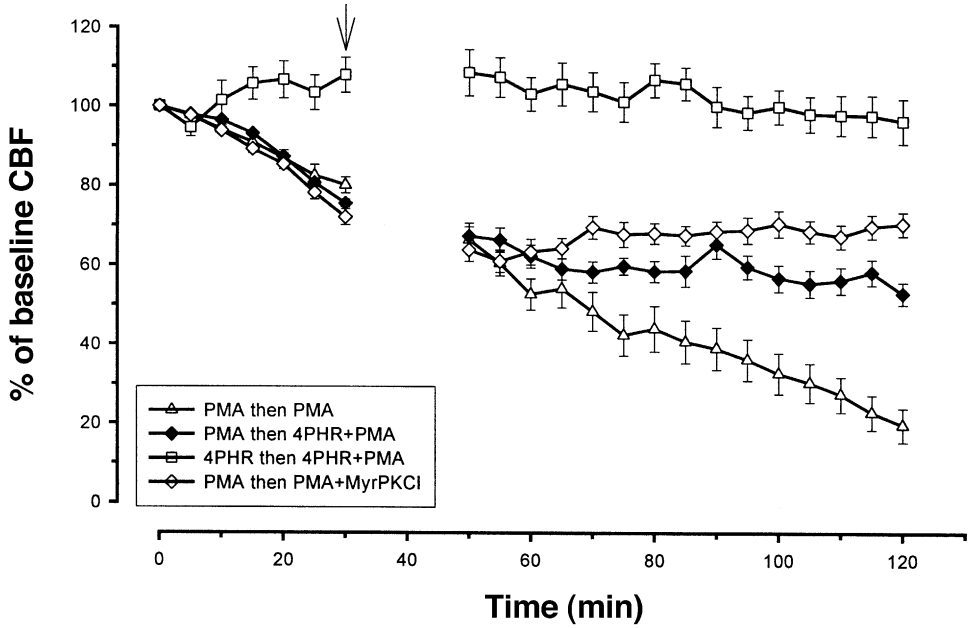

Fig. 3. CBF reaction to the presence of PMA, MyrPKCI, and 4α-PHR at 32°C. Cilia were observed for 30 min in 1 nM PMA before perfusion with different combinations of PKC modifiers at 0.125 ml min^{-1} for 20 min. For example, 1 nM PMA ($n=12$), or a mixture of either 1 nM 4α-PHR and 1 nM PMA ($n=12$), or 1 nM PMA and 10 μM MyrPKCI ($n=25$). Cilia were also observed in a 1 nM 4α-PHR solution, before perfusing the 4α-PHR+PMA mixture ($n=12$). The point at which the fresh perfusion was started is shown by the downward pointing arrow above the graph. There was a significant difference between all the profiles following the 20 min perfusion ($P<0.001$, by regression analysis).

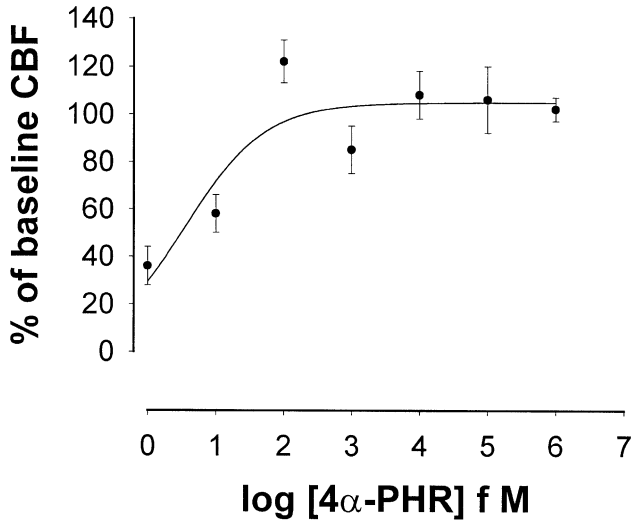

Fig. 4. A plot of data showing 4α-PHR effects on CBF in 1nM PMA at 32°C. Cilia were observed in a mixture of 1 nM PMA and various concentrations of 4α-PHR (abscissa, 0 corresponds to 10^{-15}M). The CBF (at 120 min) is expressed as percent of baseline to show the normal inhibition of CBF in the presence of PMA. 4α-PHR exerted a stabilising effect at >100 fM despite the presence of 1 nM PMA.

2 h. In order to confirm that the inhibitory effect of PMA on CBF was mediated by PKC, we kept HNE in 1 nM PMA for 30 min before perfusing 10 μM MyrPKCI+1 nM PMA. This reagent combination (Fig. 3, open diamonds, $n=25$) arrested the decline in CBF at 68 ± 3% of the baseline. Thus, we observed a highly significant difference between the post-perfusion CBF profiles in PMA alone compared to those in either the PMA+4α-PHR, or PMA+MyrPKCI ($P<0.001$). The stable CBF profile obtained when HNE were observed in 4α-PHR before perfusing the 4α-PHR+PMA mixture was also significantly different from the other profiles ($P<0.001$).

3.3. Dose responses to 4α-PHR in 1 nM PMA without flow

Having observed that 1 nM 4α-PHR prevented a decline in CBF when combined with 1 nM PMA, and that 4α-PHR reversed the decline in CBF induced by 1 nM PMA when perfused after this decline was relatively advanced, we tested the potency of the effect. A dose–response curve was constructed which gave the surprising result that 4α-PHR was cilio-active at 100 fM despite the presence of 1 nM PMA (Fig. 4). 1 nM PMA was only able to exert inhibition on CBF when the 4α-PHR was below 10 fM ($P=0.6$, by regression analysis).

The significant difference between the active and 'inactive' phorbol could result from effects on either the BIMI-insensitive, but MyrPKCI-sensitive, atypical PKC isoforms (for ex-

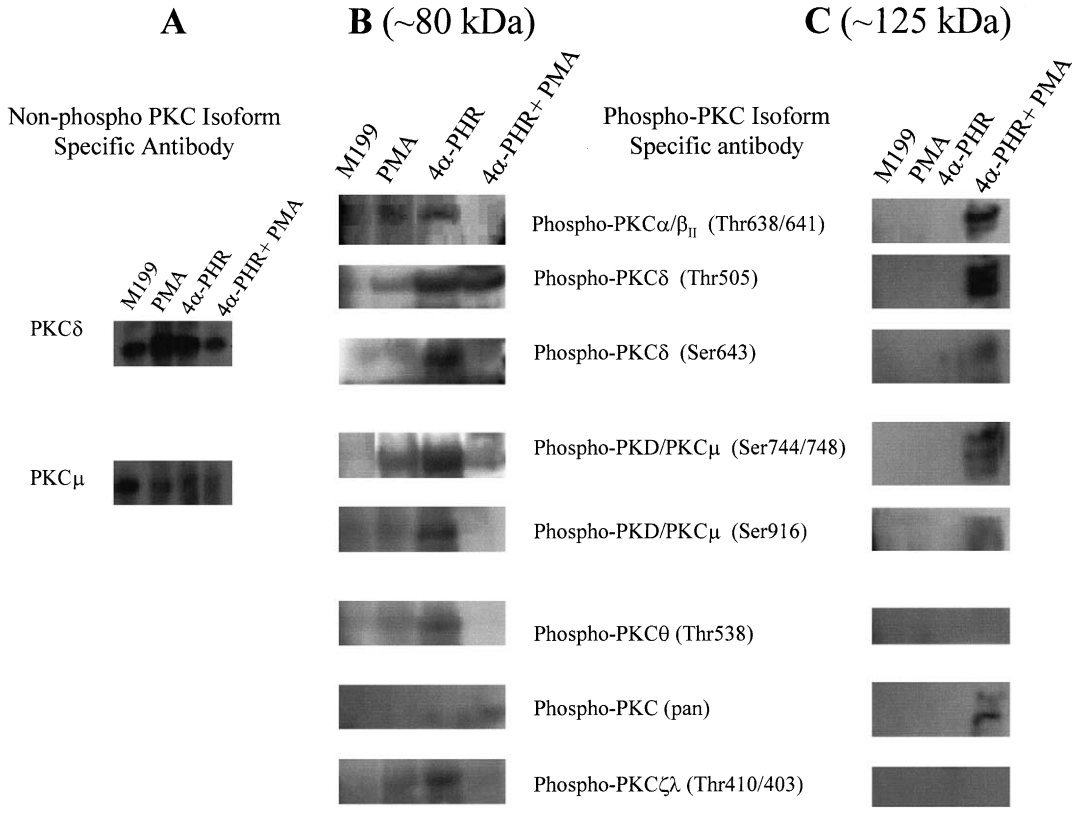

Fig. 5. The effects of 4α-PHR ± PMA on the profile of phosphorylated PKC species. A: Western blots showing the pattern of non-phospho-PKC isoform-specific staining using the antibodies indicated. For each antibody, from left to right, the four lanes shown represent typical patterns found at the expected molecular weight for most PKC species (80 kDa) after 30 min incubation with M199 alone (lane 1), +1 nM PMA (lane 2), +1 nM 4α-PHR (lane 3) or the combination of 4α-PHR+PMA (lane 4). B: The pattern of phosphorylated bands on Western blots using the anti-phospho-specific antibodies shown. C: A similar arrangement of panels but focuses on a 125 kDa protein that was only strongly phosphorylated when the combination of 4α-PHR+PMA was present.

ample PKCλ, ι, and ζ), or the other non-δ and non-ε novel PKC isoforms (PKCθ, η, μ, or PKCν). As a first step, we tested the hypothesis that 4α-PHR can alter the phosphorylation status of PKC in HNE. Western blot analysis of multiple phospho-PKC isoforms showed that the profile of phosphorylated PKC species observed with 4α-PHR differed significantly from that seen with PMA. For example, phospho-PKCθ and PKCδ (Ser643) were selectively phosphorylated in the presence of 4α-PHR compared to M199 or PMA ± 4α-PHR (Fig. 5A). No simple pattern of PKC phosphorylation could be discerned in the presence of PMA+4α-PHR because some phospho-PKC species (e.g. PKCα/βII) disappeared compared to M199 whereas others remained unchanged (e.g. PKCδ Thr505). To ascertain the significance of the changes in the phosphorylation profile, we used PKCδ and PKCμ (non-phospho) isoform-specific antibodies to determine the total endogenous PKC protein levels. Unlike the profile obtained with the phospho-PKC species, the intensity of staining for non-phospho PKCδ and PKCμ did not differ significantly between the treatments. We also observed that the combination of the two phorbol moieties resulted in the selective phosphorylation of a 125 kDa protein (Fig. 5B) that was detected by all the phospho-PKC antibodies with the exception of PKCθ and ζ/λ. That this 125 kDa protein was also detected by a pan phospho-PKC antibody (raised against a C terminal epitope common to α/βII) is suggestive that it also belongs to the PKC family despite the fact that its molecular weight is higher than that reported for most PKC species with the exception of PKD/PKCμ. We also observed that the phosphorylation of the 125 kDa protein was accompanied by the disappearance of all the lower molecular weight PKC antibody-reactive bands below 80 kDa (not shown but see PKM species in Section 4).

4. Discussion

Our approach shows how on-line measurements of ciliated cell function provide a rapid bioassay to dissect the effects of global and partial inhibition of the complex PKC enzyme family. We also show that multiple members of the PKC family are present in airway epithelium and that their phosphorylation state differs dependent on modulators of PKC function. However, further work will be needed to unravel the links between the modulators that alter the patterns of phosphorylated species and the regulation of CBF. With respect to those modulators that control CBF, we confirm that pseudosubstrate peptides such as MyrPKCI are dominantly negative over activators such as phorbol esters because they act downstream within the PKC molecule. This explains why MyrPKCI blocked the effects of PMA on CBF (Figs. 1 and 2). The effects of other modulators remain to be explained and we report three unexpected effects on the pattern of decline in CBF compared to that observed in M199. Firstly, BIMI, the selective inhibitor of classical and some novel PKC (δ and ε) isoforms [32–35] decreases CBF in a linear fashion. This decline was not seen with MyrPKCI. This difference suggests a complex interplay between PKC family members. Secondly, the 'inactive' 4α-PHR alone prevents any significant decline in CBF. This finding is especially surprising as the latter compound has been thought to be inactive with respect to PKC activity [18,19]. Thirdly, although 4α-PHR is considered to be suitable as a negative control, our results demonstrate that in whole cell HNE preparations, 4α-PHR is not neutral, but rather potently inhibits the effects of PMA on CBF. For example, administration of a concentration of 4α-PHR two log orders below that of PMA prevented the expected PMA-induced decline in CBF. Combining these findings, we suggest that the stabilising effect of 4α-PHR on CBF in the absence of PMA (and maintaining CBF above medium control) points to a latent pathway that modifies net PKC function ex vivo and our data showing that 4α-PHR can arrest the effect of PMA suggests that 4α-PHR exerts its effects on CBF by a route downstream of PMA. The exact pathway remains unknown but HNE harvested under similar conditions to the above experiments manifest a profile of phosphorylated PKC species that is altered by the presence of 4α-PHR. The simplest hypothesis is that (non-PKC) phorbol ester-binding proteins may be involved [36] in the regulation of PKC function. The extreme potency of the 4α-PHR effect might relate to the recent observation that cells contain chimaerins, proteins with high affinity phorbol-binding domains that control Rac GTPase activating protein activity with alteration of sub-cellular localisation. For example, β_2-chimaerin translocates to the Golgi apparatus after binding phorbol esters [37]. Thus, cilia might possess moieties that specifically interact with non-PKC-active phorbol esters at different sites from those responsible for interactions with PKC-active phorbols. However, we cannot exclude an interaction with the recently described 3-phosphoinositide-dependent kinase-1, which activates membrane-bound PKC [38–40] by inducing autophosphorylation at two cardinally important sites in the C1 and C2 domains within the carboxy terminus of PKC. This phosphorylation enables a given membrane-delimited form of PKC to translocate into the cytosol, where it remains inactive due to the binding of the autoinhibitory pseudosubstrate peptide. PMA liberates this latent pool of inactive PKC species by effecting the necessary conformational changes for removal of the pseudosubstrate from the activation site. Thus, our complex findings with respect to PMA and MyrPKCI might also involve differential effects on active and inactive isoforms of PKC. For example, the MyrPKCI-based CBF profiles presented here could involve PKC isoforms which contain a constitutive deletion of the inhibitory domain, such as PKCμ and PKCν. PKCμ and ν may, indeed, comprise a discrete PKC sub-group of their own [41,42]. This might underpin a constitutive activity of PKC in unstimulated ciliated cells. Another biochemical entity which is constitutively 'PKC-active', is the phorbol ester-insensitive protein kinase M family (PKM) [43–45]. PKM species are formed when the catalytically active fragment of PKC is cleaved from the parent PKC molecule at the hinge region. We note that the combination of 4α-PHR and PMA eliminated phosphorylated PKC species of smaller molecular weight than 80 kDa (not shown), moieties that are suitable candidates for PKM. It is still possible that PKM would need to be anchored to, or be near the cell membrane for the catalytic site to carry out its kinase function. This might explain the observed differences between PMA-dependent inhibition of CBF and MyrPKCI-dependent maintainence of intrinsic CBF. For example, PKM species are expected to be inhibited by MyrPKCI, but would not necessarily be activated by PMA, since the regulatory domains containing the phorbol ester-binding receptors are absent. Our speculation is that, although the PKC isoforms involved in regulating CBF would not necessarily be activated

by PMA, they could still be blocked by 4α-PHR activity acting on different phorbol-sensitive receptor sites from those on which PMA acts to regulate CBF. We conclude that allegedly inactive phorbol esters should be used with caution in physiological experiments because they may have potent effects on the prevalence of multiple phosphorylated PKC species. The study of CBF provides a relatively fast bio-assay of PKC function and may help elucidate the role of this family of enzymes in health and disease.

Acknowledgements: X.K.M. was supported by a Travelling Research Fellowship from the International Panel of the Wellcome Trust. We thank the Anonymous Trust and N. Buist for support.

References

[1] Ono, Y., Fujii, T., Igarashi, K., Kuno, T., Tanaka, C., Kikkawa, U. and Nishizuka, Y. (1989) Proc. Natl. Acad. Sci. USA 86, 4868–4871.
[2] Gschwendt, M., Kittstein, W. and Marks, F. (1991) Trends Biochem. Sci. 16, 167–169.
[3] Azzi, A., Boscoboinik, D. and Hensey, C. (1992) Eur. J. Biochem. 208, 547–557.
[4] Zhang, G., Kazanietz, M.G., Blumberg, P.M. and Hurley, J.H. (1995) Cell 81, 917–924.
[5] Hofmann, J. (1997) FASEB J. 11, 649–669.
[6] Newton, A.C. (1997) Curr. Opin. Cell Biol. 9, 161–167.
[7] Gschwendt, M. (1999) Eur. J. Biochem. 259, 555–564.
[8] Kazanietz, M.G., Caloca, M.J., Eroles, P., Fujii, T., Garcia-Bermejo, M.L., Reilly, M. and Wang, H. (2000) Biochem. Pharmacol. 60, 1417–1424.
[9] Wanner, A. (1977) Am. Rev. Respir. Dis. 116, 73–125.
[10] Sleigh, M., Blake, J.R. and Liron, N. (1988) Am. Rev. Respir. Dis. 137, 726–741.
[11] Kobayashi, K., Tamaoki, J., Sakai, N., Chiyotani, A. and Takizawa, T. (1989) Lung 167, 277–284.
[12] Salathe, M., Pratt, M.M. and Wanner, A. (1993) J. Cell Sci. 106, 1211–1220.
[13] Wong, L.B. and Yeates, D.B. (1992) Am. J. Respir. Cell Mol. Biol. 7, 447–454.
[14] Mwimbi, X.K., Muimo, R., Green, M. and Mehta, A. (2000) J. Aerosol Med. 13, 273–280.
[15] Deriemer, S.A., Strong, J.A., Albert, K.A., Greengard, P. and Kaczmarek, L.K. (1985) Nature 313, 313–316.
[16] Geiges, D., Meyer, T., Marte, B., Vanek, M., Weissgerber, G., Stabel, S., Pfeilschifter, J., Fabbro, D. and Huwiler, A. (1997) Biochem. Pharm. 53, 865–875.
[17] Hill-Venning, C. and Cottrell, G.A. (1992) Exp. Physiol. 77, 891–901.
[18] Blumberg, P.M. (1980) Crit. Rev. Toxicol. 8, 153–197.
[19] Blumberg, P.M. (1980) Crit. Rev. Toxicol. 8, 199–234.
[20] Eichholtz, T., De Bont, D.B.A., De Widt, J., Liskamp, R.M.J. and Ploegh, H.L. (1993) J. Biol. Chem. 268, 1982–1986.
[21] Harris, T.E., Persaud, S.J., Saermark, T. and Jones, P.M. (1996) Mol. Cell. Endocrinol. 121, 133–141.
[22] Harris, W., Wilkinson, S.E. and Nixon, J.S. (1997) Expert Opin. Ther. Pat. 7, 63–68.
[23] Hu, H. (1996) Drug Discov. Today 1, 438–447.
[24] Rutland, J. and Cole, P.J. (1980) Lancet 2, 564–565.
[25] Di Benedetto, G. and Mehta, A. (1990) Eur. Resp. J. 3, 257S.
[26] Rusznak, C., Devalia, J.L., Lozewicz, S. and Davies, R.J. (1994) Respir. Med. 88, 89–101.
[27] Smith, R.P., Shellard, R., Dhillon, D.P., Winter, J. and Mehta, A. (1996) J. Physiol. 496, 883–889.
[28] Di Benedetto, G., Magnus, C.J., Gray, P.A. and Mehta, A. (1991) J. Physiol. 439, 103–113.
[29] Smith, R.P., Shellard, R., Di Benedetto, G., Magnus, C.J. and Mehta, A. (1996) Eur. Respir. J. 9, 86–92.
[30] Di Benedetto, G., Lopez-Vidriero, M.T. and Clarke, S.W. (1987) Bull. Eur. Physiopathol. Respir. 23, 364S.
[31] Luk, C.M. and Dulfano, M.J. (1983) Clin. Sci. 64, 449–451.
[32] Wilkinson, S.E. and Hallam, T.J. (1994) Trends Pharm. Sci. 15, 53–57.
[33] Kiss, Z., Phillips, H. and Anderson, W.H. (1995) Biochim. Biophys. Acta 1265, 93–95.
[34] Ku, W.-C., Cheng, A.-J. and Wang, T.-C. (1997) Biochem. Biophys. Res. Commun. 241, 730–736.
[35] Wilkinson, S.E., Parker, P.J. and Nixon, J.S. (1993) Biochem. J. 294, 335–337.
[36] Caloca, M.J., Garcia-Bermejo, M.L., Blumberg, P.M., Lewin, N.E., Kremmer, E., Mischak, H., Wang, S., Nacro, K., Bienfait, B., Marquez, V.E. and Kazanietz, M.G. (1999) Proc. Natl. Acad. Sci. USA 96, 11854–11859.
[37] Caloca, M.J., Wang, H., Delemos, A., Wang, S. and Kazanietz, M.G. (2001) J. Biol. Chem. 276, 18303–18312.
[38] Chou, M.M., Hou, W., Johnson, J., Graham, L.K., Lee, M.H., Chen, C.-S., Newton, A.C., Schaufhausen, B.S. and Toker, A. (1998) Curr. Biol. 8, 1069–1077.
[39] Dutil, E.M., Toker, A. and Newton, A.C. (1998) Curr. Biol. 8, 1366–1375.
[40] Le Good, J.A., Ziegler, W.H., Parekh, D.B., Alessi, D.R., Cohen, P. and Parker, P.J. (1998) Science 281, 2042–2045.
[41] Hayashi, A., Seki, N., Hattori, A., Kozuma, S. and Saito, T. (1999) Biochim. Biophys. Acta 1450, 99–106.
[42] Schenk, P.W. and Snaar-Jagalska, B.E. (1999) Biochim. Biophys. Acta 1449, 1–24.
[43] Crossman, C.M., Mohan, P.S., Nixon, R.A. and Shea, T.B. (1995) FEBS Lett. 367, 223–227.
[44] Gallicano, G.I., McGaughey, R.W. and Capco, D.G. (1995) Dev. Biol. 167, 482–501.
[45] Ekinci, F.J. and Shea, T.B. (1999) Brain Res. 850, 207–216.